

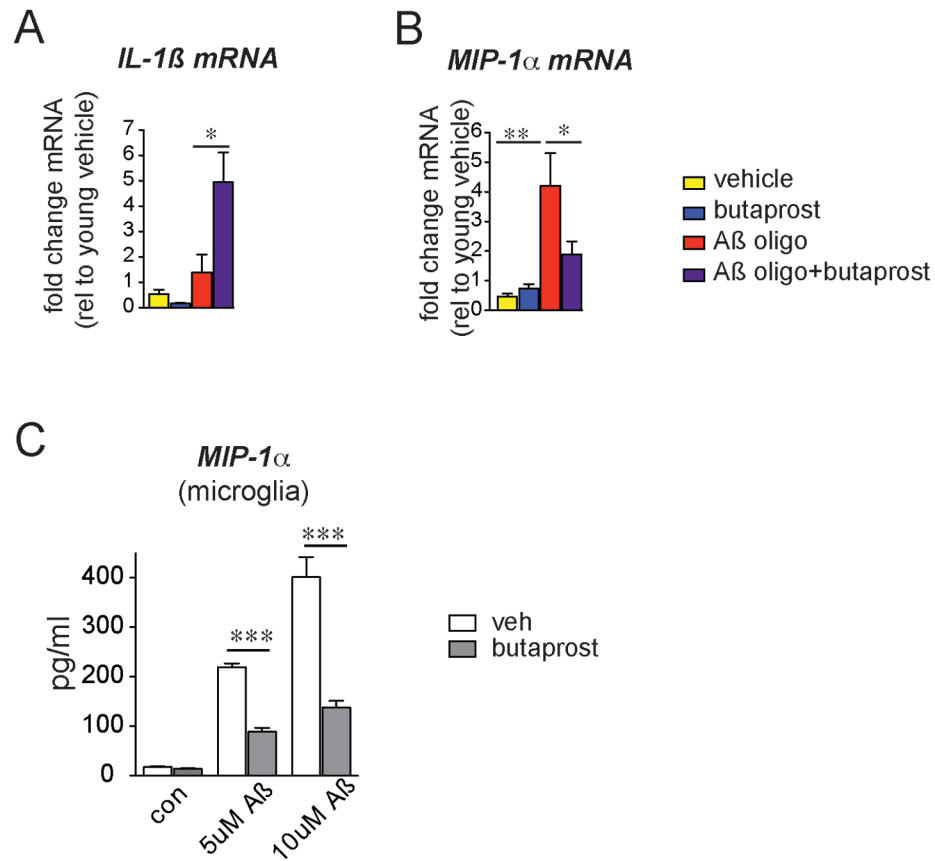
**SUPPLEMENTARY DATA FOR MANUSCRIPT:**

**PGE<sub>2</sub> EP2 signaling suppresses beneficial microglial function in AD models**

Jenny U. Johansson<sup>1,4</sup>, Nathaniel S. Woodling<sup>1, 2, 5</sup>, Qian Wang<sup>1</sup>, Maharshi Panchal<sup>1</sup>, Xibin Liang<sup>1</sup>, Angel Trueba-Saiz<sup>3</sup>, Holden D. Brown<sup>1,6</sup>, Siddhita D. Mhatre<sup>1</sup>, Taylor Loui<sup>1</sup>, and Katrin I. Andreasson<sup>1</sup>

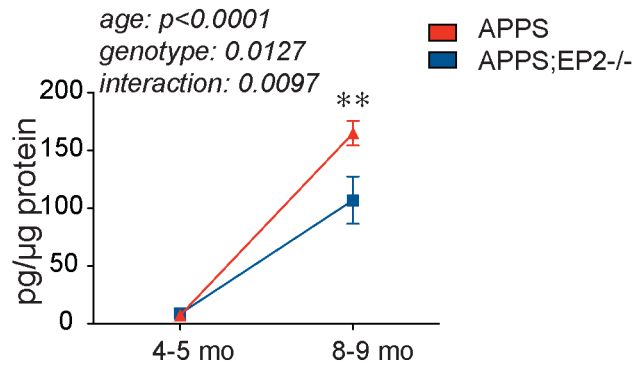
**Supplementary Table 1. qRT PCR primers**

	<b>Sense</b>	<b>Anti-sense</b>	<b>Accession Number</b>
<b>18S</b>	5'- CGGCTACCACATCCAAGGAA -3'	5'- GCTGGAATTACCGCGGCT -3'	AY248756
<b>EP2</b>	5'- TGCTGGCTTCATATTCAAGAAA -3'	5'- TGGCCAGACTAAAGAAGGTCA -3'	NM_008964
<b>COX-2</b>	5'- TGCAAGATCCACAGCCTACC -3'	5'- GCTCAGTTGAACGCCTTTTG -3'	NM_011198
<b>iNOS</b>	5'- TGACGGCAAACATGACTTCAG -3'	5'- GCCATCGGGCATCTGGTA -3'	MMU43428
<b>gp91<sup>phox</sup></b>	5'- CCAACTGGGATAACGAGTTCA -3'	5'- GAGAGTTTCAGCCAAGGCTTC -3'	NM_007807
<b>p67<sup>phox</sup></b>	5'- GCCGGAGACGCCAGAAGAGCTA -3'	5'- GGGGCTGCGACTGAGGGTGAA -3'	NM_010877
<b>p47<sup>phox</sup></b>	5'- TACAGCAAAGGACAGGACTGGGTT -3'	5'- GAGGCACTTGGCTTTCTGCAAAC -3'	NM_010876
<b>IL-1<math>\beta</math></b>	5'- CCAGGATGAGGACATGAGCACC -3'	5'- TTCTCTGCAGACTCAAACCTCCAC -3'	NM_008361
<b>MCP-1</b>	5'- TCACCTGCTGCTACTCATTACCA -3'	5'- TGAAGACCTTAGGGCAGATGCAGT -3'	NM_011333
<b>MIP-1<math>\alpha</math></b>	5'- ATACAAGCAGCAGCGAGTACCACT -3'	5'- AATCTTCCGGCTGTAGGAGAAGCA -3'	NM_011337
<b>Neprilysin</b>	5'- AGTATGCTTGTGGAGGCTGGTTGA -3'	5'- AGGTTGTCCGCCTCTGCTATCAAT -3'	NM_008604
<b>MMP-9</b>	5'- TCTTTGAGTCCGGCAGACAATCCT -3'	5'- ACACCCACATTTGACGTCCAGAGA -3'	NM_013599
<b>Insulysin</b>	5'- TGCAGAAGGACCTCAAGAATGGGT -3'	5'- GGAAACTATTGCCACCCGCACATT -3'	NM_031156
<b>Iba1</b>	5'- ATGAGCCAAAGCAGGGATTTG -3'	5'- TCTCCAGCATTTCGCTTCAAGG -3'	NM_019467
<b>CD68</b>	5'- TACAATGTGTCCTTCCCACAGGCA -3'	5'- AGGTCAAGGTGAACAGCTGGAGAA -3'	NM_009853
<b>Igf1</b>	5'- AAAGCAGCCCGCTCTATCC -3'	5'- CTTCTGAGTCTTGGGCATGTCA -3'	NM_001111274
<b>GAPDH</b>	5'- TGCACCACCAACTGCTTAG -3'	5'- GATGCAGGGATGATGTTC -3'	NM_008084

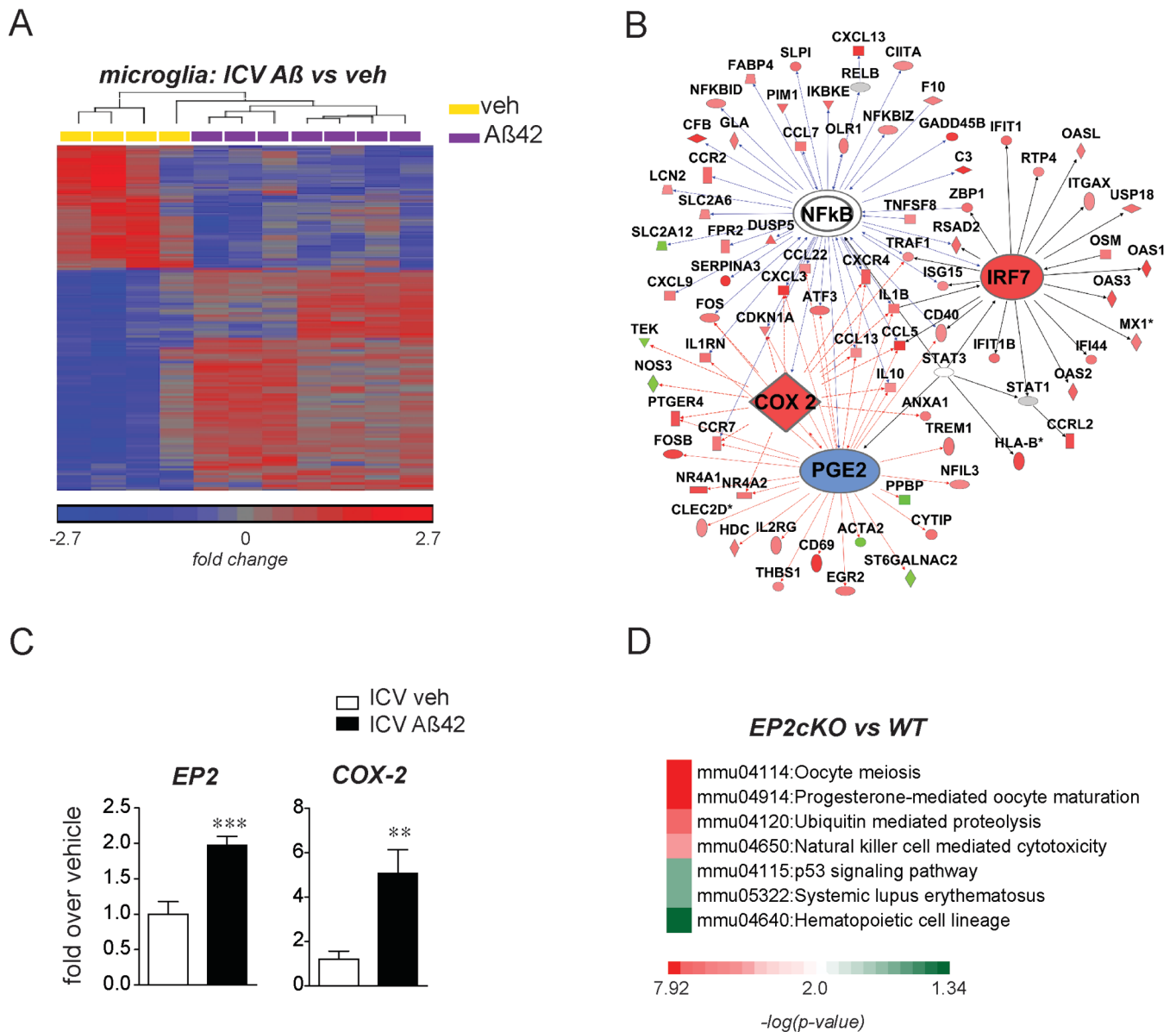


**Supplementary Figure 1. Effects of EP2 receptor activation on IL-1 $\beta$  and MIP-1 $\alpha$  expression.** Aged (21 mo) peritoneal macrophages were stimulated with A $\beta$ <sub>42</sub> oligomers (5  $\mu$ M) +/- the EP2 receptor agonist butaprost (1  $\mu$ M), and mRNA was measured by qPCR at 4 hours for **(A)** IL-1 $\beta$  and **(B)** MIP-1 $\alpha$  (n=5-6 per group, \*p<0.05 and \*\*p<0.01 by t-test). **(C)** Validation of effect of EP2 receptor activation was carried out in primary post-natal microglia. Butaprost suppresses A $\beta$ <sub>42</sub>-induced MIP-1 $\alpha$  secretion (n=4 per group; effects of A $\beta$ <sub>42</sub> and of butaprost p<0.0001; post hoc p<0.0001 for both 5  $\mu$ M and 10  $\mu$ M A $\beta$ <sub>42</sub> oligomers).

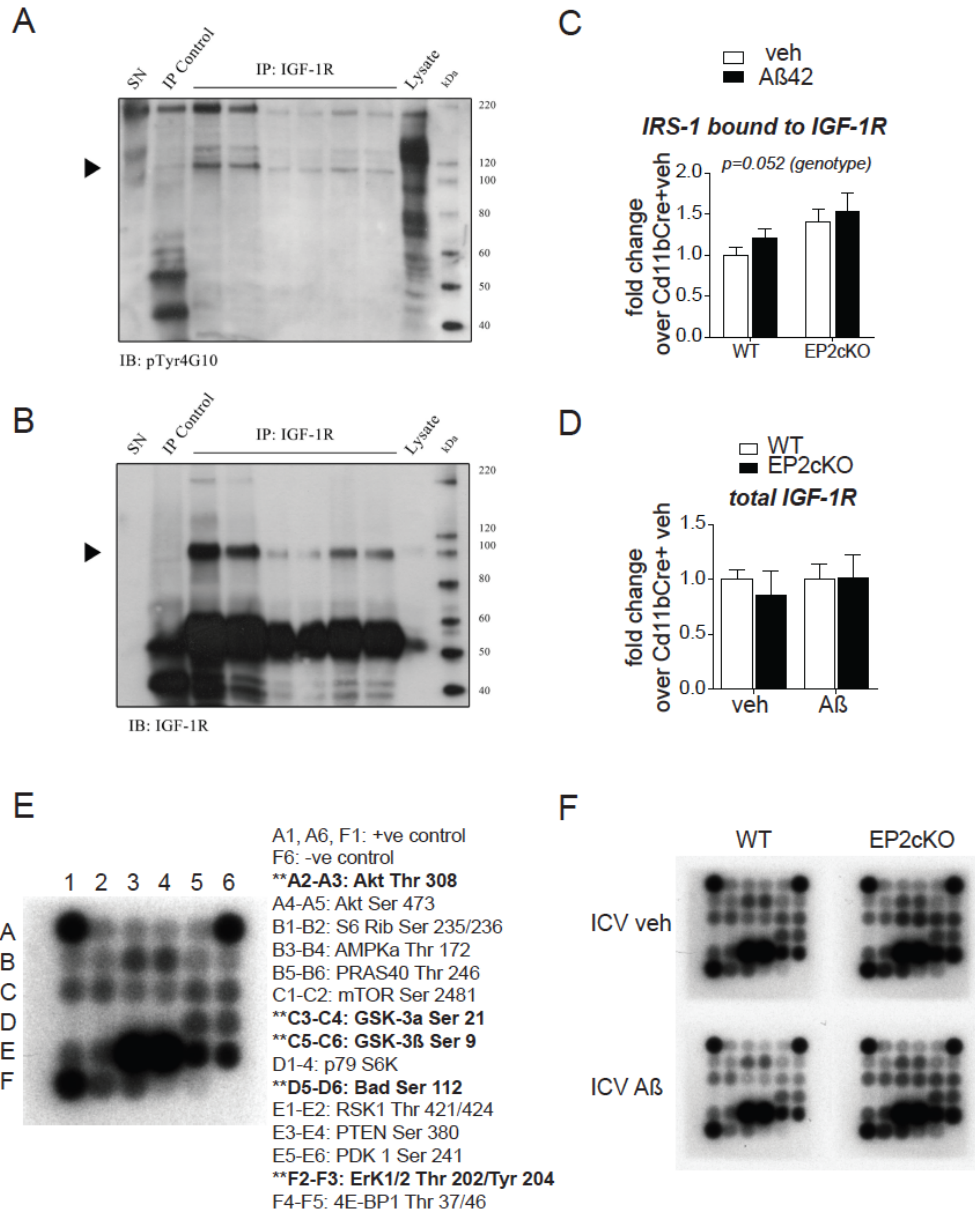
### **A $\beta$ 42 levels from 4-9 mo APP-PS1 brains**



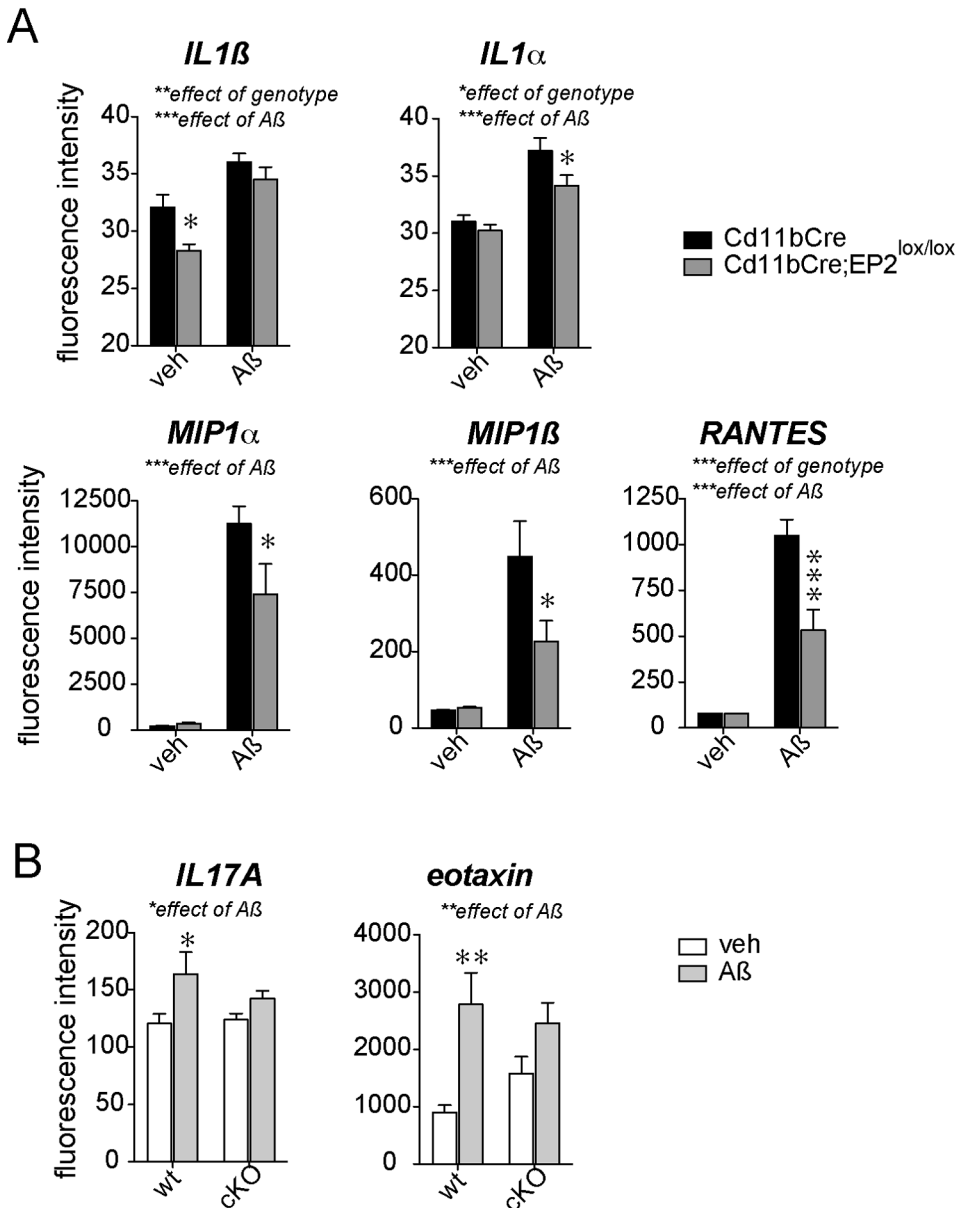
**Supplementary Figure 2. Effect of EP2 signaling on levels of A $\beta$ 42 in cerebral cortex with aging in APP-PS1 mice.** Cerebral cortex from 4-5 and 8-9 mo APP-PS1 and APP-PS1;EP2KO mice was homogenized in 5M guanidine to denature soluble and insoluble A $\beta$ <sub>42</sub> peptides; guanidine was then removed with ethanol precipitation and supernatants were assayed for A $\beta$ <sub>42</sub> by ELISA. No differences were observed at 4-5 months between genotypes, however a significant decrease was observed at 8-9 mo in APP-PS1 mice lacking EP2 (effect of genotype:  $p=0.0127$  and effect of age:  $p < 0.0001$ ; post-hoc Bonferroni  $p < 0.01$  at 8-9 mo;  $n=5-8$  per group). Previous studies have shown that this decrease is not associated with decreased generation of APP, BACE activity, or levels of  $\beta$ -CTF (1).



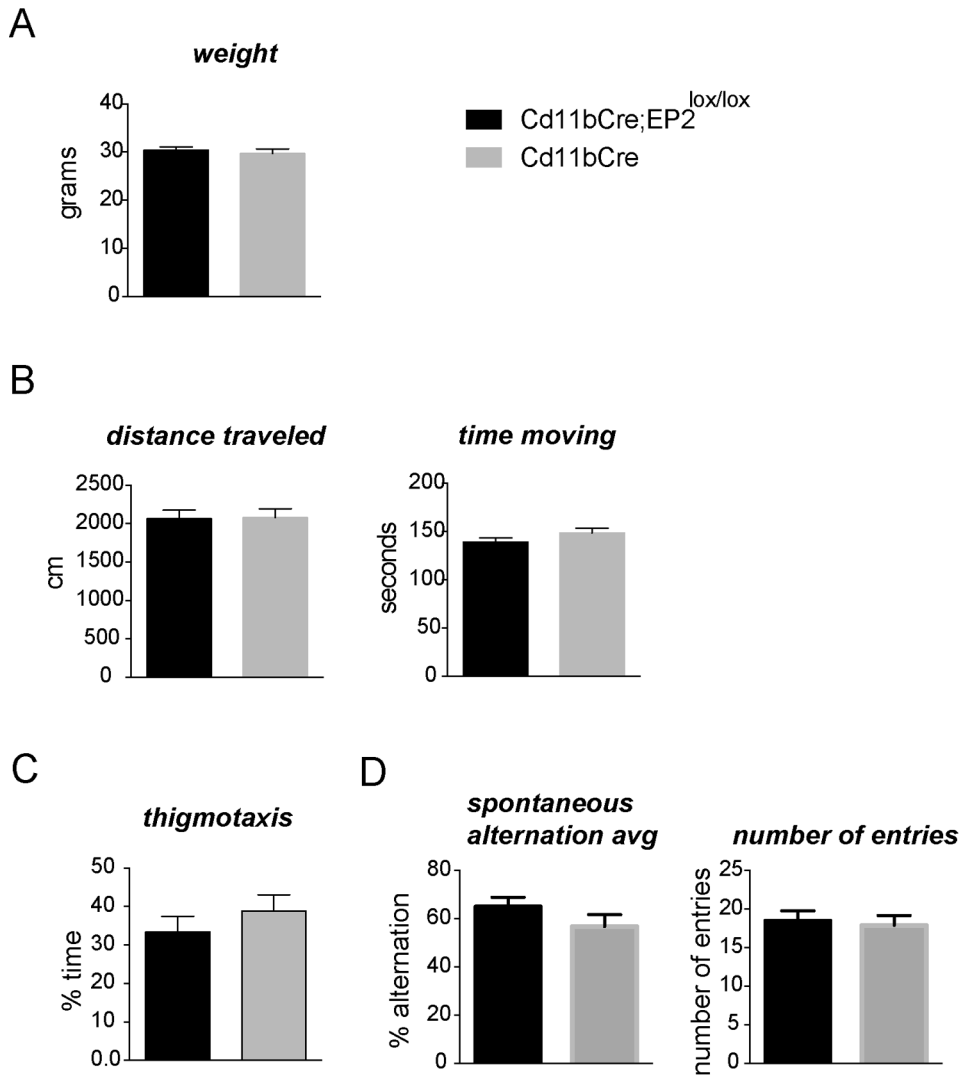
**Supplementary Figure 3. Microglial EP2 signaling regulates distinct immune and non-immune pathways.** Adult microglia were harvested from brains of 8 mo Cd11bCre;EP2<sup>+/+</sup> (WT) and Cd11bCre;EP2<sup>lox/lox</sup> (EP2cKO) mice 48h after ICV administration of vehicle or A $\beta$ <sub>42</sub> fibrillar peptides. **(A)** Hierarchical cluster analysis of differentially regulated genes in the WT+A $\beta$ <sub>42</sub> vs WT+veh comparison is shown. **(B)** Upstream regulator analysis was performed using Ingenuity Pathway Analysis (IPA) on genes regulated  $\geq 1.5$ -fold by ICV A $\beta$ <sub>42</sub> (upregulated genes in pink and red, indicating induction of 1.5-1.99 and  $\geq 2$ -fold, respectively; downregulated genes in green, representing reduction  $\geq 1.5$ -fold). NF- $\kappa$ B and IRF7, as well as COX-2 and PGE<sub>2</sub> regulate transcriptional response to A $\beta$ <sub>42</sub>. **(C)** EP2 and COX-2 mRNA are upregulated in vivo by qPCR of purified adult microglia following ICV vehicle or A $\beta$ <sub>42</sub> (n=7-8 per group; \*\*p<0.01 and \*\*\*p<0.001). **(D)** KEGG pathways, including cell cycle, proteolysis, and immune pathways, are significantly over-represented in the microglial EP2cKO vs WT comparison.



**Supplementary Figure 4. Immunoprecipitation of IGF-1R and IRS-1.** For (A) and (B), SN: supernatant, after immunoprecipitation (IP) with rabbit anti-IGF receptor antibody; IP Control: hippocampal lysate IP with rabbit serum (total IP elution volume is 40  $\mu$ l); IP IGF-1R: hippocampal lysate IP with rabbit anti-IGF-1R with lanes in duplicate (40, 10, and 20 $\mu$ l); Lysate: non immunoprecipitated lysate. IB: immunoblot. Arrowhead indicates correct molecular weight for IGF receptor and phospho-IGF receptor. (C) Immunoprecipitated IRS-1 in hippocampus at 48h is shown post ICV veh or ICV A $\beta$  (ANOVA effect of genotype,  $p=0.052$ ). (D) Levels of total IGF1 receptor normalized to actin are unchanged between genotypes and treatment groups ( $n=6-9$  per group). (E) Order of phosphoproteins in PathScan (Cell Signaling) multi-antibody array slide. Phosphoproteins marked with \*\* and bold are quantified in Figure 5D. (F) Representative array from each of the four groups quantified in Figure 5D.

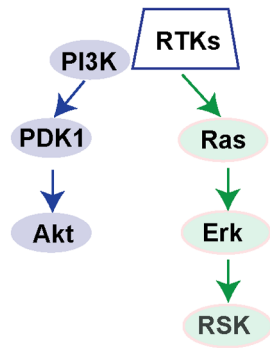


**Supplementary Figure 5. Immune factors are regulated by microglial EP2 48h following ICV A $\beta_{42}$ .** Hippocampi were harvested from brains of 8 mo Cd11bCre;EP2<sup>+/+</sup> (WT) and Cd11bCre;EP2<sup>lox/lox</sup> (EP2cKO) mice 48h after ICV administration of vehicle or A $\beta_{42}$  (n=7-8 per group). **(A)** IL1 $\beta$  (effect of genotype: \*\*p=0.0083 and effect of A $\beta$ : \*\*\*p<0.0001; post hoc Bonferroni \*p<0.05); IL1 $\alpha$  (effect of genotype:\*p=0.032 and effect of A $\beta$ : \*\*\*p<0.0001; post hoc \*p<0.05); MIP1 $\alpha$  (effect of genotype:p=0.07 and effect of A $\beta$ : \*\*\*p<0.0001; post hoc \*p<0.05); MIP1 $\beta$  (effect of genotype:p=0.06 and effect of A $\beta$ : \*\*\*p<0.0001; post hoc p<0.05); RANTES (effect of genotype:\*\*\*p=0.0009 and effect of A $\beta$ : \*\*\*p<0.0001; post hoc \*\*\*p<0.0001). **(B)** IL17A shows significant effect of A $\beta$  only in WT genotype that is suppressed in EP2cKO (effect of A $\beta$ : \*p=0.0136; post hoc \*p<0.05 for effect of A $\beta$ ); eotaxin similarly shows effect of A $\beta$  only in WT genotype (effect of A $\beta$ : \*\*p=0.0014; post hoc \*\*p<0.01 for effect of A $\beta$ ).

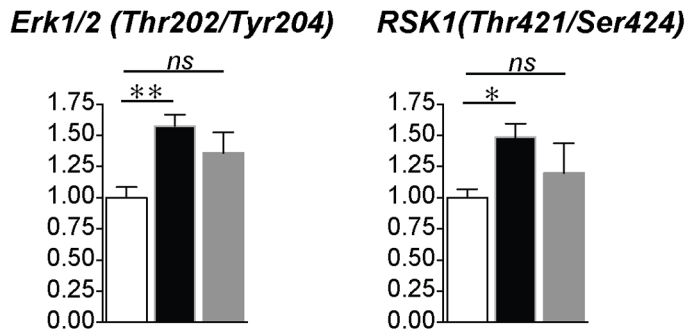


**Supplementary Figure 6. Functional characterization of microglial EP2 conditional knockout mice.** Cohorts of 3-4 mo male Cd11bCre and Cd11bCre;EP2<sup>lox/lox</sup> (n=9-10 per genotype) were examined for **(A)** weight and **(B)** distance traveled and time spent moving in an open arena over a 5 minute period. **(C)** The percent time spent moving along the periphery of the arena (thigmotaxis) over a 5 minute period was quantified as a measure of anxiety. **(D)** Y maze performance was quantified as percent spontaneous alternation (average of all trials) and number of entries (n=9-10 male 3-4 mo mice per genotype).

A



B



**Supplementary Figure 7. Regulation of Erk1/2 signaling in APP-PS1 and APP-PS1;EP2cKO cerebral cortex at 9 mo of age.** (A) Diagram of receptor tyrosine kinase (RTK) signaling pathways. (B) Phosphorylation of Erk1/2 and RSK1 is increased in APP-PS1;Cd11bCre mice compared to Cd11bCre controls. This increase is abrogated with microglial deletion of EP2 (n=4-5 per group; \*p<0.05; \*\*p<0.01).

## References

1. Liang, X., Wang, Q., Hand, T., Wu, L., Breyer, R.M., Montine, T.J., and Andreasson, K. 2005. Deletion of the prostaglandin E2 EP2 receptor reduces oxidative damage and amyloid burden in a model of Alzheimer's disease. *J Neurosci* 25:10180-10187.